Volume 6 | Number 35 | 21 September 2018 | Pages 16713–17236

# Journal of Materials Chemistry A

Materials for energy and sustainability

rsc.li/materials-a

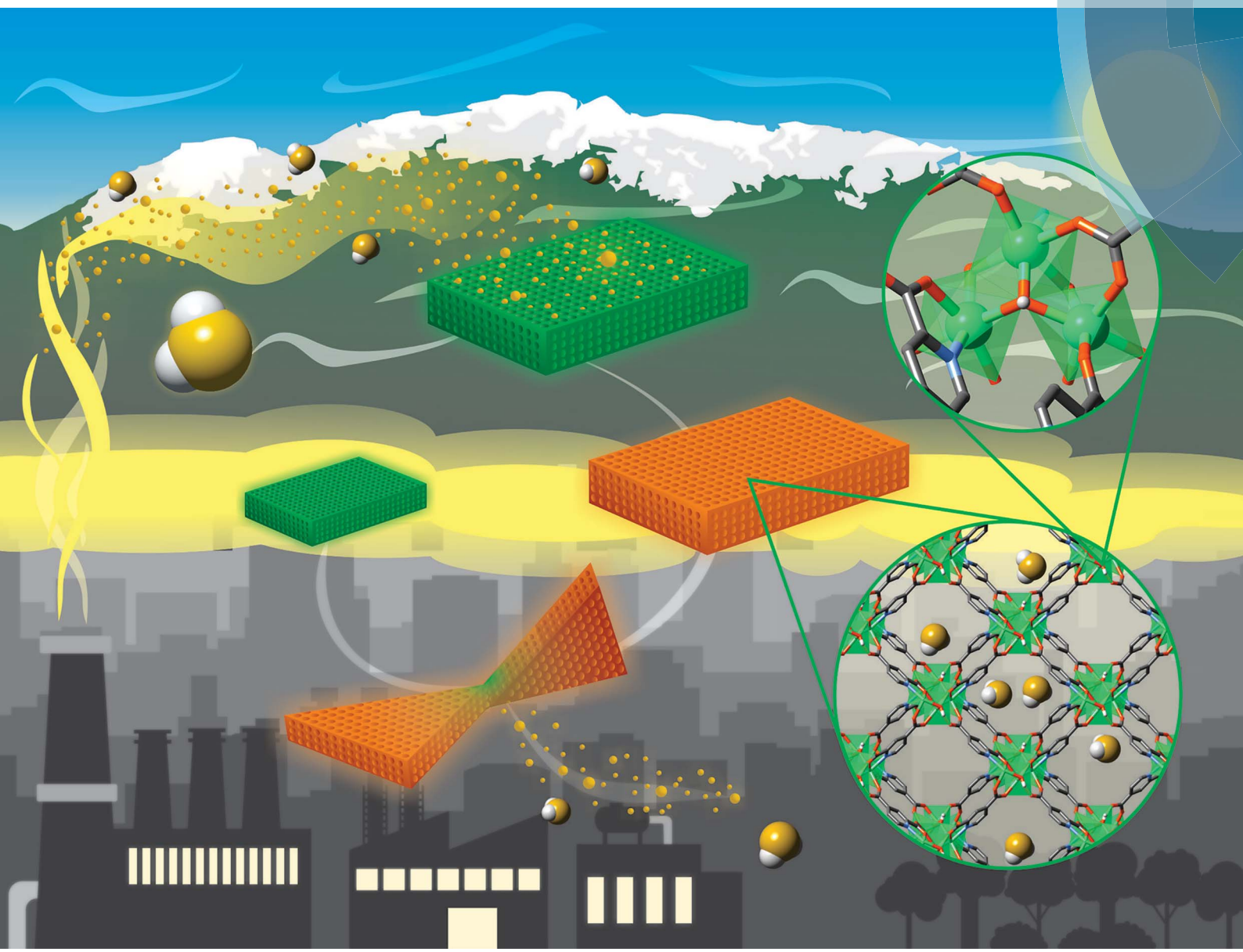

ISSN 2050-7488

ROYAL SOCIETY OF CHEMISTRY

PAPER

Guillaume Maurin, Simon M. Humphrey, Ilich A. Ibarra *et al.*
Highly reversible sorption of $H_2S$ and $CO_2$ by an environmentally friendly Mg-based MOF

Journal of Materials Chemistry A

PAPER

View Article Online
View Journal | View Issue



Cite this: J. Mater. Chem. A, 2018, 6, 16900

# Highly reversible sorption of $H_2S$ and $CO_2$ by an environmentally friendly Mg-based MOF†

Elí Sánchez-González, ‡[a] Paulo G. M. Mileo,‡[b] Mónica Sagastuy-Breña,[a] J. Raziel Álvarez,[a] Joseph E. Reynolds, III,[c] Aline Villarreal,[d] Aída Gutiérrez-Alejandre,[d] Jorge Ramírez,[d] Jorge Balmaseda,[a] Eduardo González-Zamora,[e] Guillaume Maurin,*[b] Simon M. Humphrey*[c] and Ilich A. Ibarra*[a]

Received 7th June 2018
Accepted 14th August 2018

DOI: 10.1039/c8ta05400b

rsc.li/materials-a

Mg-CUK-1, an ecologically friendly material synthesised in water is found to be a high-capacity, highly reversible adsorbent for acidic gases including $H_2S$ and $CO_2$. Furthermore, Mg-CUK-1 is demonstrated to retain long-range crystallinity upon sorption cycling; its sorption performance is maintained over multiple cycles, even in the presence of high relative humidity (95%). Reversible $H_2S$ adsorption by Mg-CUK-1 is rare among MOFs studied for this purpose to date. The joint experimental and computational studies presented here show that Mg-CUK-1 is an effective solid adsorbent for applications in the field of acid gas capture, an application that is highly relevant for the purification of many industrial gas streams.



## Introduction

The development of new functional materials for environmental remediation applications such as the capture of toxic gaseous by-products is an important issue for many large-scale industrial processes.[1] There is a continuing need to improve the performance of such materials, as well as to determine ways to manufacture them using environmentally sensitive and realistically scalable methods. Metal–Organic Frameworks (MOFs) are a topical class of crystalline solids[2a] that can be synthesised with 3-D microporous structures, making them ideal candidates for toxic gas remediation applications.[2c,b] MOFs have already shown promise in the selective capture of a variety of pollutants of direct relevance to air quality, climate change, and human health in modern society.[3] By tailoring the chemical functionality of the MOF pore environment, the sorption behaviour of a given MOF can be fine-tuned for highly selective storage and/or separation of specific gaseous pollutants, including $CO_2$,[4] $H_2S$,[5] $SO_2$,[6] $NH_3$,[7] $NO_x$,[8] and volatile organic compounds (VOCs).[3,5a,9,10] Despite their potential utility, the vast majority of MOFs must be synthesised using harmful organic solvents (*e.g.*, *N*,*N*′-dimethylformamide, DMF),[11] in direct conflict with the primary motivations of using such materials to address environmental issues. Thus, the preparation of functional MOFs using green synthetic strategies, *i.e.*, using water as a solvent and non-toxic metal and organic components, is of timely importance.[12]

Hydrogen sulfide ($H_2S$) is a toxic species present in natural gas and biogas; the desulphurisation process of different gas streams, (*e.g.*, oil refineries) is a primary source of $H_2S$ emissions.[5b] $H_2S$ is a colourless gas, which is highly corrosive, flammable and poisonous to humans. At concentrations over 100 ppm, $H_2S$ can be lethal since this molecule is quickly absorbed into the blood stream, limiting $O_2$ uptake at the cellular level.[13] Therefore, the selective capture of $H_2S$ is essential in many industrial processes. However, only very few porous materials have been comprehensively studied in $H_2S$ capture to date.[5a,b] Representative studies reported by De Weireld,[14] Zou[15] and Eddaoudi[16] indicate that most of the MOFs undergo decomposition upon adsorption of $H_2S$, while it is difficult for some others to desorb $H_2S$ due to relatively strong host-guest binding in the pores either *via* strong physisorption or even by chemisorption. In this case, desorption of $H_2S$ is therefore accompanied by an impractically large energy penalty.[17] The identification of new MOFs that are capable of highly cyclable $H_2S$ sequestration under industrially feasible pressure-swing desorption conditions[18a] remains an important,

[a]Laboratorio de Fisicoquímica y Reactividad de Superficies (LaFReS), Instituto de Investigaciones en Materiales, Universidad Nacional Autónoma de México, Circuito Exterior s/n, CU, Del. Coyoacán, 04510, Ciudad de México, Mexico. E-mail: argel@unam.mx; Fax: +52(55)-5622-4595

[b]Institut Charles Gerhardt Montpellier, UMR-5253, Université de Montpellier, CNRS, ENSCM, Place E. Bataillon, 34095 Montpellier cedex 05, France. E-mail: guillaume.maurin@univ-montp2.fr

[c]Department of Chemistry, The University of Texas at Austin, Welch Hall 2.204, 105 East 24th St., Stop A5300, Austin, Texas 78712-1224, USA. E-mail: smh@cm.utexas.edu

[d]UNICAT, Departamento de Ingeniería Química, Facultad de Química, Universidad Nacional Autónoma de México (UNAM), Coyoacán, Ciudad de México, Mexico

[e]Departamento de Química, Universidad Autónoma Metropolitana-Iztapalapa, San Rafael Atlixco 186, Col. Vicentina, Iztapalapa, C. P. 09340, Ciudad de México, Mexico

† Electronic supplementary information (ESI) available: TGA data, PXRD data, SEM micrographs, breakthrough plots, DRIFT-FTIR spectra and molecular simulations. See DOI: 10.1039/c8ta05400b

‡ These authors contributed equally to this work.

unsolved problem. $CO_2$ is another topical acidic gas that is commonly present alongside $H_2S$ in industrial gas streams (*e.g.*, in natural gas and syngas).[18b] Thus, there is a critical need to design new adsorbents that can reversibly capture both $H_2S$ and $CO_2$ with high capacities, under industrially realistic conditions.

Perhaps the most vitally important consideration regarding the potential use of MOFs as $H_2S$ and $CO_2$ adsorbents under industrially realistic conditions relates to their stability in the presence of ambient moisture. Effluent gas streams that require scrubbing for $H_2S$ and other toxic molecules commonly contain high relative humidity (% RH). This presents a major problem to MOFs that are susceptible to hydrolysis.[19a] As a potential solution to this problem, it has been shown that MOFs constructed using highly polarizing and high-valent metal cations (*e.g.*, $Mg^{2+}$, $Cr^{3+}$, $Al^{3+}$, $Ti^{4+}$, and $Zr^{4+}$) exhibit enhanced chemical stability in the presence of moisture.[19b,c] Other examples of water-stable MOFs include those recently reported by Dincă *et al.*,[19d] Eddaoudi *et al.*[19e] and Uribe-Romo *et al.*[19f] which showed outstanding water adsorption performances. Such hydrolytic stable MOFs could also be employed in a number of other critical large-scale applications, as adsorbents in heat-pumps and chillers,[20] in storage technologies for arid environments,[21] in low-cost water capture and abatement,[22] and in water-mediated proton conductors.[23]

In this contribution, we show that an environmentally friendly Mg(II)-based MOF can reversibly adsorb $H_2S$ and $CO_2$ gases with high storage capacities, between 0 and 1 bar. The MOF, called Mg-CUK-1 [24] (CUK = Cambridge University–KRICT), originally reported by Humphrey and co-workers, can be prepared rapidly (30 min) in large quantities under microwave-assisted heating, using only water as solvent.[24] Mg-CUK-1 is also of relatively low toxicity, since it is only comprised of Mg(II) ions coordinated to the commercially available organic ligand 2,4-pyridinedicarboxylic acid (2,4-pdc$H_2$; $C_5H_3N$-2,4-$CO_2H$) and hydroxide ions ($OH^-$). Mg-CUK-1 was shown to be unusually thermally stable (>500 °C) owing to the presence of infinite chains of edge- and vertex-sharing $[Mg_3(\mu_3\text{-OH})]^{5+}$ triangles that support corrugated 1-D channels with a cross-sectional accessible opening of 8.1 × 10.6 Å (Fig. 1).[24] Based on the solvent of synthesis, Mg-CUK-1 is inherently water-stable and it can be rehydrated by direct immersion in aqueous media.

In this work, to test the viability of Mg-CUK-1 in the reversible capture of the acidic gases $CO_2$ and $H_2S$ as well as the adsorption of $CO_2$ in the presence of relative humidity, we carefully characterised the following features: (i) the $H_2O$ adsorption–desorption properties to evaluate the impact of humidity on the material; (ii) the $CO_2$ capture properties under controlled RH; and, (iii) the $H_2S$ sequestration performance upon multiple cycles of adsorption and desorption. To support these application-focused experimental studies, we have employed advanced computational methods to gain fundamental insights into the mechanisms responsible for the observed reversible sorption of $H_2S$ and $CO_2$ by Mg-CUK-1 under operating conditions.

## Experimental section

### Chemicals

2,4-Pyridinedicarboxylic acid (2,4-pdc$H_2$), magnesium nitrate hydrate ($Mg(NO_3)_2$) and potassium hydroxide (KOH) were purchased from Sigma-Aldrich and used as received. In-house deionised water was used to prepare all solutions. For sorption studies, ultra-high purity (99.9995+%) $N_2$ and $CO_2$ gases as well as $H_2S$ (15.0% vol. diluted in $N_2$) were obtained from Praxair.

### Material synthesis

Mg-CUK-1, $[Mg_3(\mu_3\text{-OH})_2(2,4\text{-pdc})_2]$, was synthesised following a previously reported procedure.[24] In brief, 2,4-pdc (170 mg; 1.0 mmol) was dissolved in $H_2O$ (4.0 $cm^3$) by the addition of KOH (2.0 M; 2.0 $cm^3$), to which was added a second solution of $Mg(NO_3)_2$ hydrate (380 mg; 1.5 mmol) in $H_2O$ (4 $cm^3$) to give a viscous, opaque white slurry. The mixture was transferred into a Teflon-lined Easy-Prep (CEM Corp.) vessel and heated at 573 K

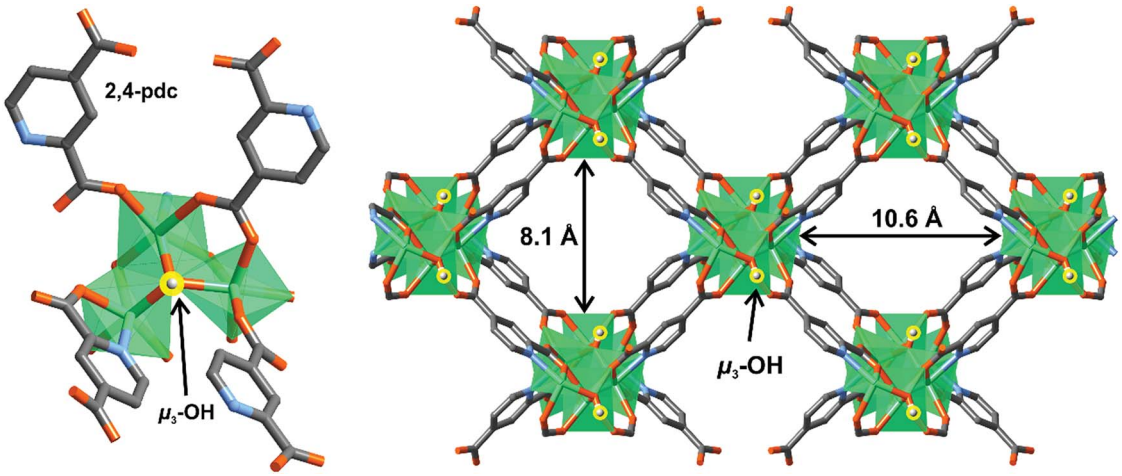


Fig. 1 (left) view of the trinuclear building block of three Mg(II) metal ions oxygen-octahedra bridged by a $\mu_3$-hydroxyl group, through the *b* axis, and (right) the crystal structure of Mg-CUK-1 along *c* axis showing 8.1 × 10.6 Å channels.

for 35 min in a MARS microwave reactor (CEM Corp.). The reaction temperature was controlled using a fiber-optic sensor. After cooling to room temperature (15–30 min), the crystalline solid was purified by short (3 × 20 s) cycles of sonication in fresh $H_2O$, followed by decanting off the amorphous suspension. Large, colourless prismatic crystals were isolated (average yield = 124 mg, 42%). Thermogravimetric analysis (TGA) and powder X-ray diffraction (PXRD) of the sample were carried out to confirm phase purity of the Mg-CUK-1 (Fig. S1 and S2†).

### Adsorption isotherms for $CO_2$ and $H_2O$

$CO_2$ sorption isotherms (196 K and up to 1 bar) were obtained on a Belsorp HP analyser under high vacuum in a clean system. The estimated BET area ($0.005 < P/P_0 < 0.15$) was equal to 604 $m^2\ g^{-1}$ with a corresponding pore volume of 0.22 $cm^3\ g^{-1}$ (Fig. S3†). These textural properties are in good agreement with the previously reported data.[24,25] This correlation confirmed the correct activation of the material. High pressure $CO_2$ adsorption isotherms (0–6 bar, and 303 K) were collected on a Belsorp HP analyser. $H_2O$ vapour isotherms were recorded by a dynamic method, using air gas as carrier gas, using a DVS Advantage 1 instrument from Surface Measurement Systems (mass sensitivity: 0.1 μg, Relative Humidity (RH), accuracy: 0.5% RH, vapour pressure accuracy: 0.7% $P/P_0$. Mg-CUK-1 samples were activated at 373 K for 1 hour under flowing $N_2$. The $H_2O$ uptake in weight percent (wt%) units was calculated as [(adsorbed amount of water)/(amount of adsorbent) × 100], consistent with established procedures. Water cycling experiments were performed at 303 K; for the adsorption phase, RH = 95% was maintained for 8 hours. Then, the sample was exposed to a dry air flow for a further 8 hours to ensure complete desorption prior to re-adsorption. $CO_2$ adsorption experiments at fixed RH were performed on the hydrated Mg-CUK-1 (13% RH). The material was activated as described above and then exposed to this constant RH for 1 hour. The water-impregnated sample was then transferred to a Belsorp HP analyser cell for the $CO_2$ adsorption.

### $H_2S$ adsorption–desorption studies

Dynamic adsorption experiments were performed at 303 K using a tubular quartz adsorber (internal diameter = 7 mm) filled with Mg-CUK-1 (Scheme S1†). Before beginning the $H_2S$ adsorption tests, samples were activated *in situ* at 373 K for 1 hour with a constant flow of dry $N_2$ gas and then slowly cooled to 303 K. Samples were exposed to synthetic $H_2S/N_2$ gas mixtures at $p = 0.689$ bar with a total flow rate = 30 $cm^3\ min^{-1}$. A HP-5890 gas chromatograph equipped with an HP-PLOT 1 column and a TCD was used to analyse the $H_2S$ concentration. Adsorption experiments at different $H_2S$ concentrations were performed using 6, 9, 12 and 15% vol $H_2S/N_2$ gas mixtures (see ESI† for the corresponding breakthrough curves). The adsorption capacities were obtained by integrating the areas above the breakthrough curves. At the end of each experiment, the Mg-CUK-1 sample was exposed to a constant flow of dry $N_2$ gas, after which the sample was put through a Temperature Swing Reactivation (TSR) cycle (under $N_2$ gas) at 373 K using the standard protocol (*vide supra*) prior to changing the $H_2S$ vol%.

### DRIFTS

Diffuse-reflectance infrared Fourier-transform spectroscopy (DRIFTS) of Mg-CUK-1 samples in powder form were performed using a Nicolet 380 spectrometer (DTGS detector) with 4 $cm^{-1}$ resolution equipped with a diffuse reflectance vacuum cell fitted with KBr windows. DRIFT spectra were collected on an activated Mg-CUK-1 sample (373 K for 1 h and $\sim 6 \times 10^{-3}$ torr), as well as of the same sample after exposure to five cycles of $H_2S$ adsorption–desorption. To do so, the as-synthesised Mg-CUK-1 was first activated and exposed to $H_2S$ using the protocol described above; after the fifth reactivation, the powder was transferred to a quartz cell and briefly evacuated at $6 \times 10^{-3}$ torr at 303 K before collecting the spectrum.

### Scanning electron microscopy (SEM)

Morphology studies were carried out on a JEOL Benchtop Scanning Electron Microscope, Neoscope JCM-6000 using secondary electrons at 15 kV current, in a high vacuum, and the processing of the images was carried out using Neoscope software.

### Computational details

The crystal structure of Mg-CUK-1 [24] (CCDC-1024710) was geometry-optimised at the density functional theory (DFT) level while keeping the experimental cell parameter fixed. These calculations employed a PBE functional[26] combined with a double numeric basis set containing polarisation functions (DNP),[27a] as implemented in the Dmol$^3$ package. The same settings were employed to geometry-optimise the $H_2S$-loaded Mg-CUK-1 at different guest concentrations. The partial charges (Fig. S6†) for each atom in the MOF were derived from the REPEAT strategy (see ESI†).[27b]

The microscopic models of the three guest molecules were defined as follows: (i) $CO_2$ was described by the EPM2 model,[28] corresponding to a rigid and linear molecule representation with 3 charged Lennard-Jones (LJ) sites and a C═O bond length of 1.149 Å; (ii) $H_2O$ was represented by the TIP4P/2005 model,[29] a four-site model, with a single LJ site centered in the oxygen position and three charged sites, two centered in the hydrogen positions and one located 0.1546 Å below the hydroxyl-O atom in the molecule bisector axis, having an O–H bond length of 0.9572 Å; and (iii) $H_2S$ was represented by the model reported by Kamath *et al.* (2005),[30] *i.e.*, using a model with three charged LJ sites centered in the atomic position, a S–H bond of 1.34 Å, and an H–S–H bond angle = 92.5°. Regarding Mg-CUK-1, the 12-6 LJ parameters for the inorganic and organic moieties were taken from the UFF[31] and DREIDING[32] force fields, respectively. The Mg-CUK-1/guest interactions were described using a 6-12 LJ potential and a coulombic contribution. Following a general approach adopted in previous studies,[33] the H atom of the $\mu_3$-OH groups interacts with the guests only through electrostatic interactions. The LJ crossed parameters between the MOF and the guests were calculated using the Lorentz–Berthelot mixing rules. The LJ contribution had a cut-off distance of 12 Å, while long-range electrostatic interactions were handled using the Ewald summation technique.[34]

 

Next, Grand Canonical Monte Carlo (GCMC) simulations were carried out at 303 K to predict the adsorption behaviour of Mg-CUK-1 for $H_2O$, $CO_2$ and $H_2S$ as single components. A simulation box made of 12 unit cells ($3 \times 2 \times 2$) was employed, by fixing all atoms of the framework in their initial positions. The adsorption enthalpies at low coverage were calculated using the revised Widom test particle insertion method.[35] As a further step, in order to gain insight into the $CO_2$ adsorption properties of Mg-CUK-1 in the presence of $H_2O$, GCMC simulations were performed for a MOF framework loaded with 1 $H_2O$ molecule per unit cell (corresponding to the experimental water loading at 13% RH). In the case of $H_2S$, additional MC simulations were performed in the canonical ensemble (NVT) to identify the preferential adsorption sites for the guest molecules at low, intermediate and high pressures. This exploration involved the analysis of the radial distribution functions plotted between different MOF/guest pairs calculated from hundreds of MC configurations.

## Results and discussion

Fig. 2A shows the water adsorption isotherm of Mg-CUK-1 between 0 and 95% $P/P_0$, obtained at 303 K. The isotherm corresponds to a Type-V adsorption behaviour: at low pressure (0–20% $P/P_0$) $H_2O$ adsorption is very gradual (Fig. 2A, inset); then, there is a rapid increase in $H_2O$ uptake between 20 and 35% $P/P_0$; above 35% $P/P_0$ the uptake remained basically constant corresponding to a maximum $H_2O$ uptake of 34.4 wt% (19.1 mmol $g^{-1}$ at 95% $P/P_0$). This performance is among the best MOF performances reported so far (adsorption uptake ranging from 25 to 40 wt%)[21,36,37] for low-cost atmospheric water generation, although the material $Co_2Cl_2$BTDD has achieved 96 wt%.[38]

These experimental data obtained for Mg-CUK-1 are in excellent agreement with the GCMC-predicted adsorption isotherm (Fig. 2A; solid line), which provides a solid validation of the microscopic model (LJ parameters and charges) employed in our simulations for the CUK-1 framework. Such a shape of the adsorption isotherm is due to the mildly hydrophilic character of Mg-CUK-1, as confirmed by a moderate simulated adsorption enthalpy for $H_2O$ at very low coverage ($-42.6$ kJ $mol^{-1}$) which then increases up to $-60$ kJ $mol^{-1}$ above $P/P_0 = 0.20$. Furthermore, one can observe a well-pronounced hysteresis loop upon desorption (Fig. 2A; open circles) mostly caused by the presence of strong H-bonding between the $H_2O$ adsorbates and the hydroxyl groups that are present once the pore starts to be filled.[39] Since the accessible pore openings of Mg-CUK-1 (8.1 × 10.6 Å)[24] are significantly larger than the kinetic diameter of $H_2O$ (2.7 Å), the observed hysteresis is unlikely to be due to the `kinetic trapping' behaviour.[40–42]

To investigate the $H_2O$ adsorption–desorption cyclability of Mg-CUK-1, a set of eight $H_2O$ sorption isotherms were measured continuously on the same sample at 303 K (Fig. 2B). This study showed no apparent decrease in the total capacity, indicating that Mg-CUK-1 can be repeatedly fully dehydrated. Water was successfully removed between each cycle by simply flowing dry $N_2$ through the sample, without the need to use additional external heating. This method of regeneration is highly beneficial from an energy economy perspective. PXRD analysis of the same Mg-CUK-1 sample after eight adsorption–desorption experiments confirmed retention of bulk crystallinity (Fig. 3; blue data). Additionally, a $CO_2$ adsorption isotherm at 196 K was collected on the sample that underwent 8 water adsorption cycles to assess the retention of its surface area under this operating condition (Fig. S4†). The estimated BET area was equal to 586 $m^2$ $g^{-1}$, which is very similar to the value obtained for the pristine material (604 $m^2$ $g^{-1}$), *i.e.* only a 3% loss of surface area. This emphasises the exceptional stability of Mg-CUK-1 in the presence of water vapour.

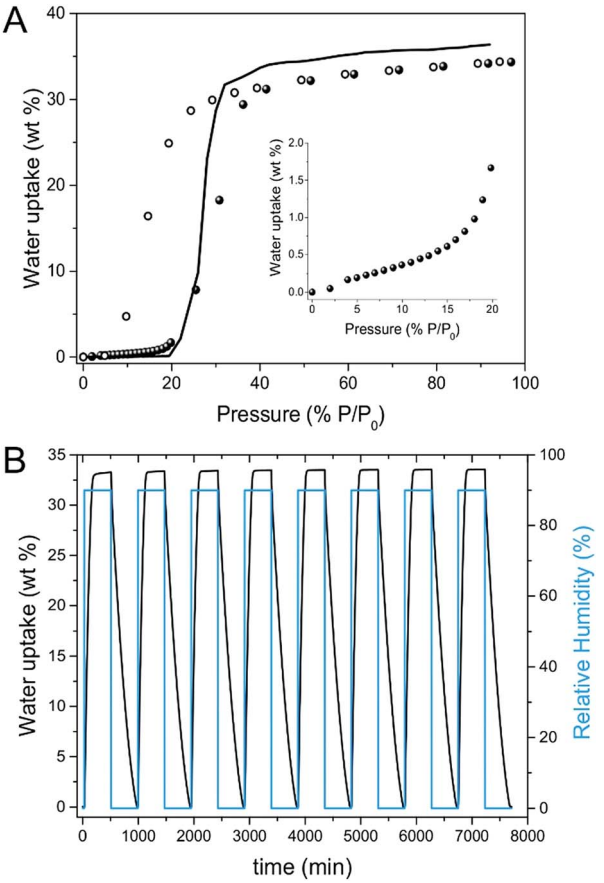


Fig. 2 (A) Water adsorption isotherm at 303 K of Mg-CUK-1 from % $P/P_0 = 0$ to 95. Solid and open circles represent experimental adsorption and desorption branches, respectively, and the solid line represents the GCMC simulations of the adsorption. The inset shows the $H_2O$ adsorption isotherm at 303 K from % $P/P_0 = 0$ to 20. (B) Water adsorption–desorption uptake obtained from 8 cycles on Mg-CUK-1 at 303 K.

### $CO_2$ adsorption studies

Next, isothermal $CO_2$ adsorption experiments were performed on Mg-CUK-1 as a function of % RH. A comparison of the $CO_2$ adsorption isotherms at 303 K obtained for the fully dehydrated Mg-CUK-1 *versus* Mg-CUK-1 rehydrated to 13% RH is presented in Fig. 4. The total adsorbed amount of $CO_2$ was very similar in both cases between 0 and 0.3 bar. At higher partial pressures,

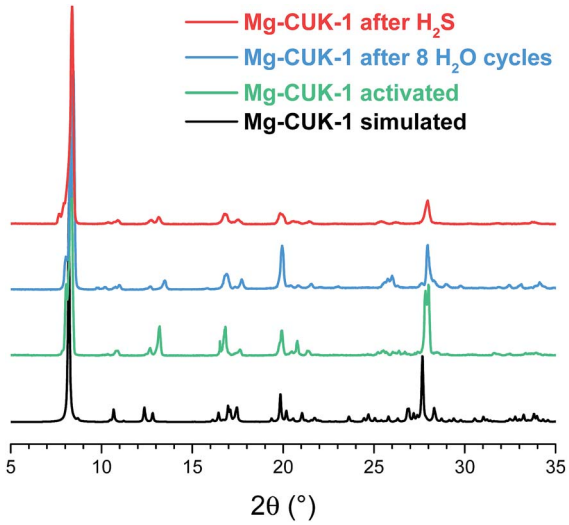


Fig. 3 PXRD patterns of the Mg-CUK-1 simulated pattern from the crystal structure (black line), activated sample (green line), after $H_2O$ sorption cycling (blue line), and after $H_2S$ sorption (red line).

there was a slight enhancement in $CO_2$ uptake for the sample at 13% RH, which reaches 3.37 mmol $g^{-1}$ at 1 bar (*cf.* 3.03 mmol $g^{-1}$ for the anhydrous sample at the same pressure; Fig. 4). At elevated pressures (2–6 bar of $CO_2$), the uptake difference remained approximately constant, reaching a total uptake of 5.89 and 6.39 mmol $g^{-1}$ for the anhydrous and partially hydrated samples, respectively. Both experimental adsorption isotherms were very well reproduced by our GCMC simulations, from which we were also able to extract a relatively high $CO_2$ adsorption enthalpy of −35 and −36.5 kJ $mol^{-1}$ for the anhydrous and partially hydrated samples, respectively; these magnitudes are in-line with what has been reported experimentally and theoretically for other $\mu_3$-OH-decorated MOFs that show specific interactions between these hydroxyl groups and the $CO_2$ molecules.[43] Interestingly, these results clearly demonstrated that the $CO_2$ adsorption properties of Mg-CUK-1 in terms of both $CO_2$ uptake and affinity are retained in the presence of humidity. This is in sharp contrast with some other $CO_2$ adsorbents which show a drastic drop of their performances in the presence of humidity.[44] We can assume that the adsorbed water binds to the $\mu_3$-OH groups that create additional adsorption sites for $CO_2$ molecules and hence contribute to slightly enhance both $CO_2$ adsorption capacity and affinity as previously observed.[39] This renders Mg-CUK-1 as an attractive adsorbent to operate the capture of $CO_2$ under real conditions.

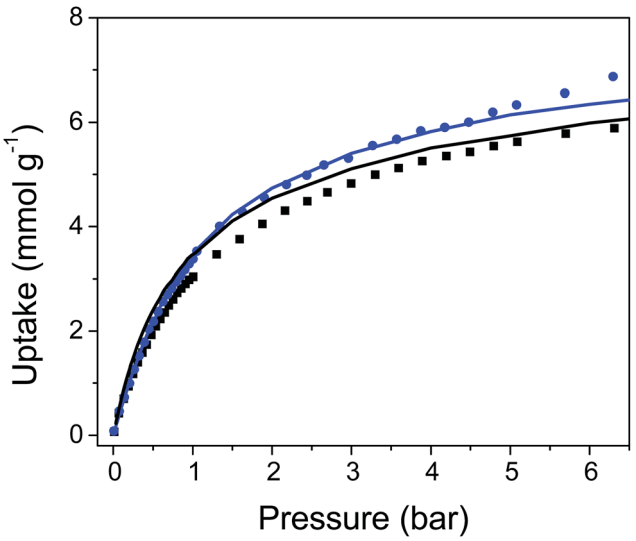


Fig. 4 Experimental $CO_2$ adsorption isotherm for fully dehydrated Mg-CUK-1 (black squares) and Mg-CUK-1 in the presence of 13% RH (blue circles); the corresponding simulated adsorption isotherms are represented as solid lines. All data are reported at 303 K.

### $H_2S$ adsorption studies

The adsorption of $H_2S$ by Mg-CUK-1 was assessed by a series of breakthrough experiments (see ESI†). The adsorption capacities obtained are shown in Fig. S8.† At the lowest $H_2S$ concentration studied (6% vol $H_2S$), the gas uptake was equal to 1.41 mmol $H_2S$ $g^{-1}$, which corresponds to 45.5 $cm^3$ $H_2S$ $g^{-1}$. This value is approximately the same as the $N_2$ adsorption capacity observed at the same pressure.[24] The $H_2S$ uptake by Mg-CUK-1 was approximately 40% higher than the performances of a number of well-studied MOFs (experiments with low $H_2S$ concentrations *ca.* 1–6 kPa), including MIL-100(Fe),[15] MIL-53(Fe),[14] HKUST-1,[15] MOF-5,[15] MIL-53(Cr),[14] Ga-soc-MOF[16] and MIL-125(Ti),[45] all of which show $H_2S$ capacities of approximately 1 mmol $g^{-1}$. Similar $H_2S$ capacities have been reported for Zn-MOF-74 (1.64 mmol $g^{-1}$)[15] and Cu(BDC)(TED)$_{0.5}$ (1.65 mmol $g^{-1}$).[15] Notably, of this entire list of MOFs, only MIL-53(Cr) and Ga-soc-MOF were able to reversibly adsorb $H_2S$ in addition to Mg-CUK-1, which is an essential condition for their potential use in practical applications. In order to validate our experimental $H_2S$ breakthrough adsorption results, we evaluated the $H_2S$ adsorption performances of MOF-74, HKUST-1 and MIL-101(Cr), which were previously explored using $H_2S$ breakthrough experiments. Our home-made experimental setup revealed very similar $H_2S$ capture performances to the existing data (see Fig. S9 and Table S2†), demonstrating the reliability of our measurements.

Interestingly, Mg-CUK-1 also exhibited a two-fold increase in its $H_2S$ adsorption capacity as the $H_2S$ feed gas concentration was increased from 6 to 15% vol (reaching 3.1 mmol $H_2S$ $g^{-1}$); 15 vol% is the maximum feed concentration that could be practically measured (equivalent to 0.1 bar of $H_2S$). In order to investigate the $H_2S$ regeneration-capacity and the structural stability of Mg-CUK-1, cycling $H_2S$ experiments at 15% vol $H_2S$ were then performed on the same Mg-CUK-1 sample; this was accompanied by PXRD and scanning electron microscopy (SEM) analyses of the products to confirm retention of the crystal structure (Fig. 3 red data and Fig. S13†). First, cycling adsorption–desorption results showed that the $H_2S$ adsorption capacity remained constant during the five adsorption–desorption cycles (3.2 ± 0.2 mmol $g^{-1}$, Fig. 5A), which suggests that $H_2S$ was completely desorbed when the sample was re-activated. A comparison of the DRIFTS data for the as-synthesised Mg-CUK-1

 

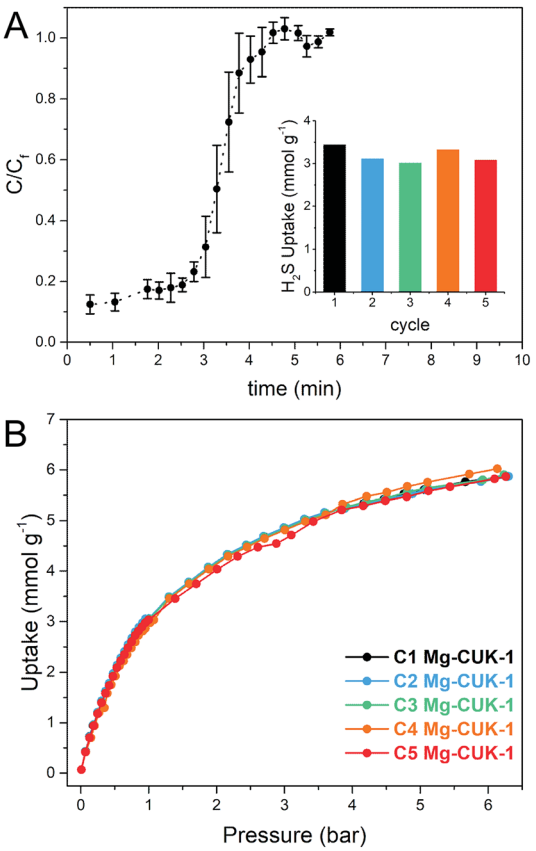


Fig. 5 (A) Breakthrough curves of $H_2S$ adsorption by Mg-CUK-1 at 303 K using a feed $H_2S$ concentration of 15% vol. The total $H_2S/N_2$ rate flow was 30 cm$^3$ min$^{-1}$. The inset shows the comparative adsorption capacities for each cycle. (B) The $CO_2$ adsorption isotherms for Mg-CUK-1 after $H_2S$ sorption cycling, measured at 303 K and up to 6.5 bar.

and $H_2S$-cycled Mg-CUK-1 samples after re-activation (at 373 K for 1 h under flowing $N_2$ gas) led to spectra that were essentially indistinguishable (Fig. S15†), confirming that this re-activation condition allows full removal of $H_2S$. Since the adsorption capacity did not change after several adsorption–desorption cycles, Mg-CUK-1 appears to be very stable upon repeated $H_2S$ exposure at room temperature. This is a desirable property for highly $H_2S$ stable MOFs; previous studies of a series of related MIL materials (MIL-47(V), MIL-53(Al, Cr),[14] and MIL-125(Ti))[45] led to the hypothesis that $H_2S$ stability is enhanced for MOFs that do not contain open metal sites, which cannot undergo M–$SH_2$ ligation. Additionally, $CO_2$ adsorption isotherms at 196 and 303 K were measured after each $H_2S$ exposure, prior to a TSR step (Fig. S10†). These experiments confirmed the retention of both the surface area (592.4 ± 7.6 m$^2$ g$^{-1}$, Fig. S12†) and the $CO_2$ adsorption capacity of the Mg-CUK-1 (5.93 ± 0.12 mmol g$^{-1}$, Fig. 5B).

As shown previously, Mg-CUK-1 demonstrates a 'soft crystalline' behaviour, being flexible in the solid-state;[46] the pores relax upon $H_2O$ adsorption/desorption.[24] Thus, we decided to investigate such a flexible behaviour when $H_2S$ molecules are adsorbed in the pores of Mg-CUK-1. First, a fully dehydrated Mg-CUK-1 was saturated with $H_2S$ (15% vol $H_2S$). Later, this sample was incompletely re-activated (by only flowing dry $N_2$ gas at 303 K for 10 minutes) to achieve a partially $H_2S$ saturated sample. When PXRD experiments were performed, a shift in the position of the low-angle reflections (between 8 and 9° 2$\theta$) was observed (see Fig. 6A). This suggested the flexible character of the structure upon $H_2S$ adsorption/desorption, since the PXRD pattern (partially $H_2S$ saturated) matched neither with the fully activated sample nor the water saturated sample (Fig. 6).

In order to gain a better understanding of the degree of flexibility of Mg-CUK-1 upon $H_2S$ loading, the experimental PXRD patterns collected at different $H_2S$ loadings were analysed

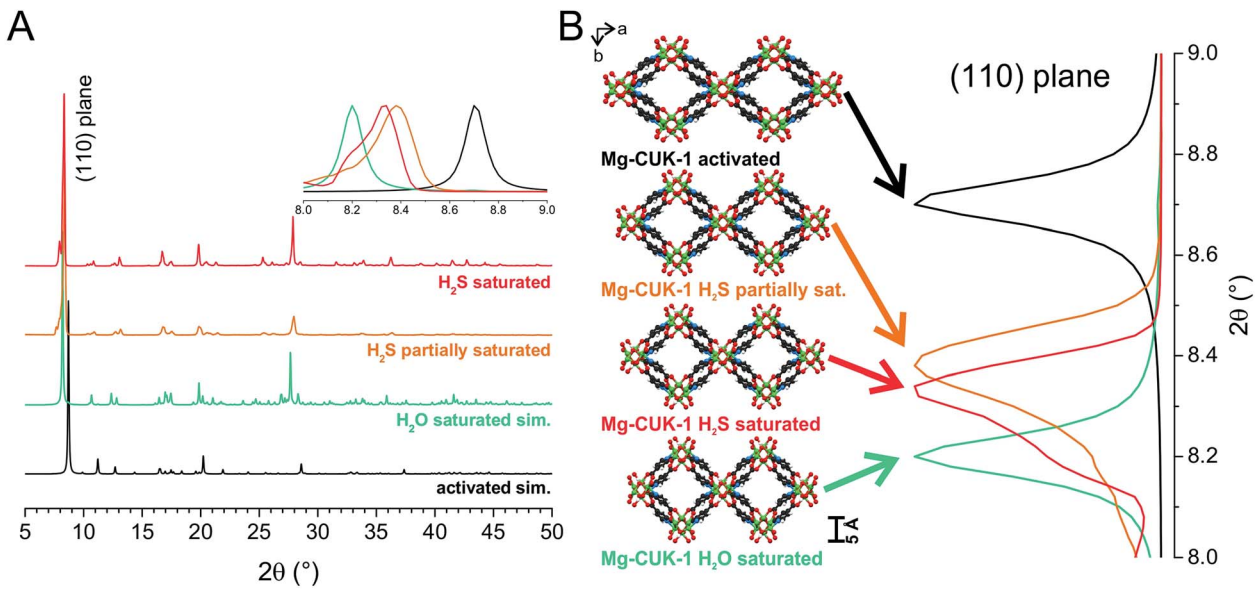


Fig. 6 (A) PXRD experiments on samples of Mg-CUK-1 with different molecule loadings. The inset shows the two-theta shifting of the 110 plane. (B) Representation of the Mg-CUK-1 cell deformation as a visual aid to explain the two-theta shifting.

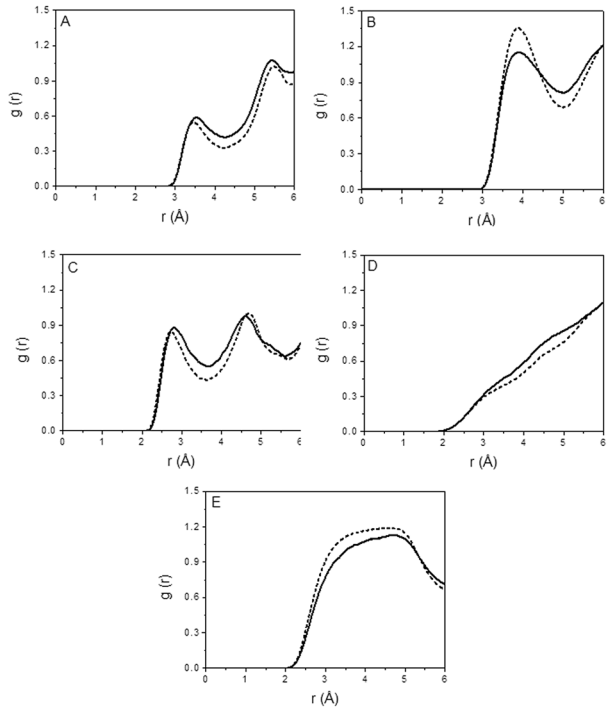


Fig. 7 Radial distribution functions for the pairs $O_{\mu_3\text{-}OH}$–S (A), $O_{carb}$–S (B), $H_{\mu_3\text{-}OH}$–S (C), $O_{\mu_3\text{-}OH}$–$H_{H_2S}$ (D), and $S_{H_2S}$–$H_{H_2S}$ (E) in Mg-CUK-1 loaded with 1.08 (solid lines) and 4.89 (dashed lines) molecules of $H_2S$ per unit cell at 303 K.

to extract the cell parameters of the $H_2S$-loaded material by the Le Bail methodology (FullProf program; see ESI†).[47] From the cell parameters derived, plausible structural models for the partially and fully $H_2S$ loaded phases were constructed starting with the crystal structure of the empty Mg-CUK-1 followed by a DFT-geometry optimisation keeping the experimental cell parameters fixed. These calculations were performed using the same functional and basis set employed to initially geometry-optimise the crystal structure of Mg-CUK-1.

Analysis of these plausible structural models indicated that the guest-induced evolution of the channel dimensions of Mg-CUK-1 (taking into consideration the van der Waals radius of the atoms, see ESI†) is as follows: fully desolvated = 9.1 × 10.3 Å; $H_2O$ saturated = 10.2 × 9.4 Å; partially $H_2S$ loaded = 9.5 × 10.1 Å; $H_2S$ saturated = 10.0 × 9.1 Å (Fig. 6B). This trend is also consistent with an increase of the unit cell volume of the structure upon adsorption: fully desolvated = 2428.4 $Å^3$; partially $H_2S$ loaded = 2518.0 $Å^3$; $H_2O$ saturated = 2543.3 $Å^3$; $H_2S$ saturated = 2541.6 $Å^3$, corresponding to about 5% guest-induced unit cell volume change.

Finally, GCMC simulations were performed to gain in-depth insights into the adsorption of $H_2S$ at the microscopic level. The calculated adsorption isotherm gave a maximum uptake of 5 mmol $g^{-1}$, which is somewhat higher than the experimentally observed value of 3.1 mmol $g^{-1}$. Our calculations further predicted an enthalpy of −23.3 kJ $mol^{-1}$ for low-coverage adsorption, which is similar to the value reported for MIL-68(Al), another hydroxyl-based MOF material.[48] This moderately strong interaction is primarily ascribed to interactions between $H_2S$ molecules and the hydroxyl groups and O-atoms of the carboxylate groups, as confirmed by the plots of the radial distribution functions (RDFs; Fig. 7A and B), which yield characteristic contact distances ranging from 3.3 Å to 4.0 Å. A corresponding snapshot showing the most preferential positions of $H_2S$ molecules within the pores of Mg-CUK-1 at low coverage (1.08 $H_2S$ per unit cell) is shown in Fig. 8A. The RDF plots in Fig. 7C and D show that the interactions between the hydroxyl groups and the $H_2S$ molecules are established through relatively weak hydrogen bonds, in which the hydroxyls are the strongest hydrogen donor. This moderate $H_2S\cdots$Mg-CUK-1 interaction is consistent with the relatively easy regeneration of the material after $H_2S$ exposure and hence the reversible adsorption of this molecule. Upon increasing the theoretical $H_2S$ loading from 1.08 to 4.89 molecules per unit cell, the calculated $\mu_3$-OH$\cdots SH_2$ distance only slightly shortened from 2.8 Å to 2.7 Å. Further, our calculations predicted that at higher $H_2S$ loading, inter-

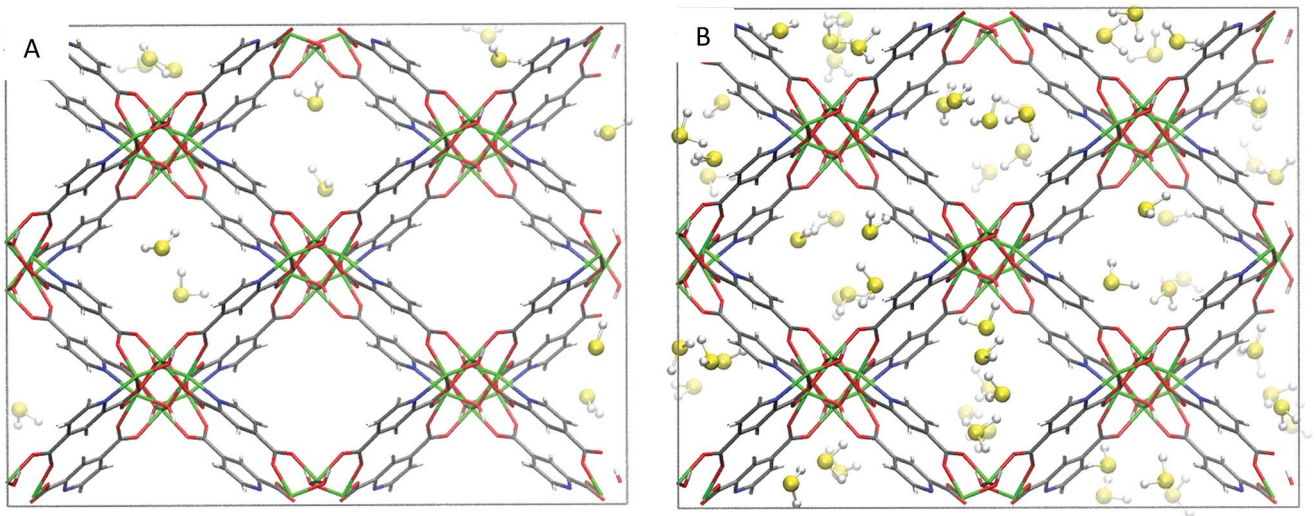


Fig. 8 (A) Representative snapshots obtained from the GCMC simulations, showing the interactions between $H_2S$ and the atoms of the MOF pore wall for 1.08 $H_2S$ per unit cell; (B) the corresponding image for a higher loading of 4.89 $H_2S$ per unit cell.

 

molecular $H_2S$ interactions tend to become slightly weaker (Fig. 7E and 8B). This finding can be attributed to a certain degree of interaction of the $H_2S$ molecules with the MOF pore-wall, which acts to prevent $H_2S$ condensation inside the micropores, as shown in MIL-47(V).[14b]

## Conclusions

The environmentally friendly synthesised Mg-CUK-1 was demonstrated to be a highly robust MOF for acid gas remediation applications. Its chemical stability towards $H_2O$ and $H_2S$ (retention of the framework crystallinity and total gas adsorption capacity) was experimentally established by powder X-ray diffraction and adsorption–desorption ($H_2O$ and $H_2S$) experimental cycles. Mg-CUK-1 is one of the best performing $H_2S$ breakthrough materials showing remarkable $H_2S$ reversibility, under temperature swing re-activation (TSR) conditions. Remarkably the $CO_2$ adsorption properties of Mg-CUK-1 remain unchanged upon exposure to $H_2O$ and $H_2S$. Mg-CUK-1 was shown to exhibit a 'soft crystalline' behaviour when small amounts of $H_2S$ are confined within its micropores. Molecular simulations complemented our experimental evidence and more importantly, provided us the preferential adsorption sites for the $CO_2$ and $H_2S$ molecules inside the channels of Mg-CUK-1. Particularly, the calculated moderate adsorption enthalpy for $H_2S$ ($-23.3$ kJ mol$^{-1}$) in comparison to exiting MOF materials confirmed the regeneration viability of Mg-CUK-1, under mild conditions. In summation, Mg-CUK-1 has been demonstrated to be an exceptional candidate for the capture of $CO_2$, even under humid conditions, as well as a remarkably stable adsorbent for the reversible sorption of $H_2S$.

## Conflicts of interest

There are no conflicts of interest.

## Acknowledgements

The authors thank Dr A. Tejeda-Cruz (powder X-ray; IIM-UNAM) for analytical assistance, U. Winnberg (ITAM) for scientific discussions and G. Ibarra-Winnberg for conceptualising the design of this contribution. Financial support for this work was provided by PAPIIT UNAM Mexico (IN101517), CONACyT under grant No. 1789 (I. A. I.), 236879 (E. G.-Z.), 276862 (J. R. Á.) and 289042 (E. S.-G.), a scholarship from the National Counsel of Technological and Scientific Development CNPQ (P. G. M. M.), the Institut Universitaire de France (G. M.), and the Welch Foundation (F-1738, J. E. R. & S. M. H.).

## Notes and references

1 P. Kumar, K.-H. Kim, E. E. Kwon and J. E. Szulejko, *J. Mater. Chem. A*, 2016, **4**, 345.

2 (*a*) G. Maurin, C. Serre, A. Cooper, G. Férey and S. L. James, *Chem. Soc. Rev.*, 2017, **46**, 3104; (*b*) S. L. James, *Chem. Soc. Rev.*, 2003, **32**, 276; (*c*) J. L. C. Rowsell and O. M. Yaghi, *Microporous Mesoporous Mater.*, 2004, **73**, 3.

3 N. M. Padial, E. Quartapelle Procopio, C. Montoro, E. López, J. E. Oltra, V. Colombo, A. Maspero, N. Masciocchi, S. Galli, I. Senkovska, S. Kaskel, E. Barea and J. A. R. Navarro, *Angew. Chem., Int. Ed.*, 2013, **52**, 8290.

4 (*a*) K. Sumida, D. L. Rogow, J. A. Mason, T. M. McDonald, E. D. Bloch, Z. R. Herm, T. H. Bae and J. R. Long, *Chem. Rev.*, 2012, **112**, 724; (*b*) J. Liu, P. K. Thallapally, B. P. McGrail, D. R. Brown and J. Liu, *Chem. Soc. Rev.*, 2012, **41**, 2308; (*c*) D. Andirova, C. F. Cogswell, Y. Lei and S. Choi, *Microporous Mesoporous Mater.*, 2016, **219**, 276.

5 (*a*) E. Barea, C. Montoro and J. A. R. Navarro, *Chem. Soc. Rev.*, 2014, **43**, 5419; (*b*) M. S. Shah, M. Tsapatsis and J. I. Siepmann, *Chem. Rev.*, 2017, **117**, 9755.

6 (*a*) D. Britt, D. Tranchemontagne and O. M. Yaghi, *Proc. Natl. Acad. Sci. U. S. A.*, 2008, **105**, 11623; (*b*) C. A. Fernandez, P. K. Thallapally, R. K. Motkuri, S. K. Nune, J. C. Sumrak, J. Tian and J. Liu, *Cryst. Growth Des.*, 2010, **10**, 1037; (*c*) T. G. Glover, G. W. Peterson, B. J. Schindler, D. Britt and O. M. Yaghi, *Chem. Eng. Sci.*, 2011, **66**, 163; (*d*) S. Yang, J. Sun, A. J. Ramirez-Cuesta, S. K. Callear, W. I. F. David, D. P. Anderson, R. Newby, A. J. Blake, J. E. Parker, C. C. Tang and M. Schröder, *Nat. Chem.*, 2012, **4**, 887; (*e*) K. Tan, P. M. Canepa, W. Gong, J. Liu, D. H. Johnson, A. Dyevoich, P. K. Thallapally, T. Thonhauser, J. Li and Y. J. Chabal, *Chem. Mater.*, 2013, **25**, 4653; (*f*) W. P. Mounfield III, C. Han, S. H. Pang, U. Tumuluri, Y. Jiao, S. Bhattacharyya, M. R. Dutzer, S. Nair, Z. Wu, R. P. Lively, D. S. Sholl and K. S. Walton, *J. Phys. Chem. C*, 2016, **120**, 27230; (*g*) K. Tan, S. Zuluaga, H. Wang, P. M. Canepa, K. Soliman, J. Cure, J. Li, T. Thonhauser and Y. J. Chabal, *Chem. Mater.*, 2017, **29**, 4227; (*h*) S. Glomb, D. Woschko, G. Makhloufi and C. Janiak, *ACS Appl. Mater. Interfaces*, 2017, **9**, 37419.

7 (*a*) K. Vikrant, V. Kumar, K.-H. Kim and D. Kukkar, *J. Mater. Chem. A*, 2017, **5**, 22877; (*b*) J. F. Van Humbeck, T. M. McDonald, X. Jing, B. M. Wiers, G. Zhu and J. R. Long, *J. Am. Chem. Soc.*, 2014, **136**, 2432; (*c*) A. J. Rieth and M. Dincă, *J. Am. Chem. Soc.*, 2018, **140**, 3461.

8 (*a*) X. Zhang, W. Chen, W. Shi and P. Cheng, *J. Mater. Chem. A*, 2016, **4**, 16198; (*b*) A. C. McKinlay, B. Xiao, D. S. Wragg, P. S. Wheatley, I. L. Megson and R. E. Morris, *J. Am. Chem. Soc.*, 2008, **130**, 10440; (*c*) M. J. Ingleson, R. Heck, J. A. Gould and M. J. Rosseinsky, *Inorg. Chem.*, 2009, **48**, 9986; (*d*) A. C. McKinlay, J. F. Eubank, S. Wuttke, B. Xiao, P. S. Wheatley, P. Bazin, J.-C. Lavalley, M. Daturin, A. Vimont, G. De Weireld, P. Horcajada, C. Serre and R. E. Morris, *Chem. Mater.*, 2013, **25**, 1592; (*e*) S. R. Miller, E. Alvarez, L. Fradxourt, T. Devic, S. Wuttke, P. S. Wheatley, N. Steunou, C. Bonhomme, C. Gervais, D. Laurencin, R. E. Morris, A. Vimont, M. Daturi, P. Horcajada and C. Serre, *Chem. Commun.*, 2013, **49**, 7773; (*f*) R. R. Haikal, C. Hua, J. J. Perry IV, D. O'Nolan, I. Syed, A. Kumar, A. H. Chester, M. J. Zaworotko, M. H. Yacoub and M. H. Alkordi, *ACS Appl. Mater. Interfaces*, 2017, **9**, 43520.

9 (*a*) L. Zhou, X. Zhang and Y. Chen, *Mater. Lett.*, 2017, **197**, 224; (*b*) K. Vellingiri, J. E. Szulejko, P. Kumar, E. E. Kwon, K.-H. Kim, A. Deep, D. W. Boukhvalov and R. J. C. Brown, *Sci. Rep.*, 2016, **6**, 27813.

10 (*a*) J.-R. Li, R. J. Kuppler and H.-C. Zhou, *Chem. Soc. Rev.*, 2009, **38**, 1477; (*b*) D. Banerjee, A. J. Cairns, J. Liu, R. K. Motkuri, S. K. Nune, C. A. Fernandez, R. Krishna, D. M. Strachan and P. K. Thallapally, *Acc. Chem. Res.*, 2015, **48**, 211; (*c*) K. Adil, Y. Belmabkhout, R. S. Pillai, A. Cadiau, P. M. Bhatt, A. H. Assen, G. Maurin and M. Eddaoudi, *Chem. Soc. Rev.*, 2017, **46**, 3402.

11 R. P. Pohanish, *Sittig's Handbook of Toxic and Hazardous Chemicals and Carcinogens*, William Andrew Publishing, New York, USA, 2008.

12 P. T. Anastas and J. C. Warner, *Green Chemistry: Theory and Practice*, Oxford University Press, Oxford, U.K., 1998.

13 (*a*) R. O. Beauchamp, J. S. Bus, J. A. Popp, C. J. Boreiko, D. A. Andjelkovich and P. Leber, *CRC Crit. Rev. Toxicol.*, 1984, **13**, 25; (*b*) P. K. Moore and M. Whiteman, *Chemistry, Biochemistry and Pharmacology of Hydrogen Sulfide*, Handbook of Experimental Pharmacology, Springer International Publishing, Switzerland, 2015.

14 (*a*) L. Hamon, C. Serre, T. Devic, T. Loiseau, F. Millange, G. Férey and G. De Weireld, *J. Am. Chem. Soc.*, 2009, **131**, 8775; (*b*) L. Hamon, H. Leclerc, A. Ghoufi, L. Oliviero, A. Travert, J.-C. Lavalley, T. Devic, C. Serre, G. Férey, G. De Weireld, A. Vimont and G. Maurin, *J. Phys. Chem. C*, 2011, **115**, 2047.

15 J. Liu, Y. Wei, P. Li, Y. Zhao and R. Zou, *J. Phys. Chem. C*, 2017, **121**, 13249.

16 Y. Belmabkhout, R. S. Pillai, D. Alezi, O. Shekhah, P. M. Bhatt, Z. Chen, K. Adil, S. Vaesen, G. De Weireld, M. Pang, M. Suetin, A. J. Cairns, V. Solovyeva, A. Shkurenko, O. El Tall, G. Maurin and M. Eddaoudi, *J. Mater. Chem. A*, 2017, **5**, 3293.

17 R.-T. Yang, in *Gas Separation by Adsorption Processes*, Imperial College Press, London, 1997, ch. 2, pp. 9–26.

18 (*a*) G. Liu, V. Chernikova, Y. Liu, K. Zhang, Y. Belmabkhout, O. Shekhah, C. Zhang, S. Yi, M. Eddaoudi and W. J. Koros, *Nat. Mater.*, 2018, **17**, 283; (*b*) M. Tagliabue, D. Farrusseng, S. Valencia, S. Aguado, U. Ravon, C. Rizzo, A. Corma and C. Mirodatos, *Chem. Eng. J.*, 2009, **155**, 553.

19 (*a*) E. González-Zamora and I. A. Ibarra, *Mater. Chem. Front.*, 2017, **1**, 1471; (*b*) T. Devic and C. Serre, *Chem. Soc. Rev.*, 2014, **43**, 6097; (*c*) A. J. Howarth, Y. Liu, P. Li, Z. Li, T. C. Wang, J. T. Hupp and O. K. Farha, *Nat. Rev. Mater.*, 2016, **1**, 15018; (*d*) C. R. Wade, T. Corrales-Sanchez, T. C. Narayan and M. Dincă, *Energy Environ. Sci.*, 2013, **6**, 2172; (*e*) S. M. T. Abtab, D. Alezi, P. M. Bhatt, A. Shkurenko, Y. Belmabkhout, H. Aggarwal, Ł. J. Weselinski, N. Alsadun, U. Samin, M. N. Hedhili and M. Eddaoudi, *Chem*, 2018, **4**, 94; (*f*) M. W. Logan, J. D. Adamson, D. Le and F. J. Uribe-Romo, *ACS Appl. Mater. Interfaces*, 2017, **9**, 44529.

20 (*a*) F. Meunier, *Appl. Therm. Eng.*, 2013, **61**, 830; (*b*) C. Janiak and S. K. Henninger, *Chimia*, 2013, **67**, 419.

21 H. Furukawa, F. Gándara, Y.-B. Zhang, J. Jiang, W. L. Queen, M. R. Hudson and O. M. Yaghi, *J. Am. Chem. Soc.*, 2014, **136**, 4369.

22 (*a*) J. Liu, F. Zhang, X. Zou, G. Yu, N. Zhao, S. Fan and G. Zhu, *Chem. Commun.*, 2013, **49**, 7430; (*b*) M. Sánchez-Serratos, P. A. Bayliss, R. A. Peralta, E. González-Zamora, E. Lima and I. A. Ibarra, *New J. Chem.*, 2016, **40**, 68.

23 (*a*) M. Sadakiyo, T. Yamada and H. Kitagawa, *J. Am. Chem. Soc.*, 2014, **136**, 13166; (*b*) M. Sadakiyo, T. Yamada, K. Honda, H. Matsui and H. Kitagawa, *J. Am. Chem. Soc.*, 2014, **136**, 7701; (*c*) P. Ramaswamy, N. E. Wong and G. K. H. Shimizu, *Chem. Soc. Rev.*, 2014, **43**, 5913; (*d*) P. Ramaswamy, N. E. Wong, B. S. Gelfand and G. K. H. Shimiz, *J. Am. Chem. Soc.*, 2015, **137**, 7640; (*e*) S. S. Nagarkar, S. M. Unni, A. Sharma, S. Kurungot and S. K. Ghosh, *Angew. Chem.*, 2014, **126**, 2676; (*f*) D. D. Borges, S. Devautour-Vinot, H. Jobic, J. Ollivier, F. Nouar, R. Semino, T. Devic, C. Serre, F. Paesani and G. Maurin, *Angew. Chem., Int. Ed.*, 2016, **55**, 3919; (*g*) P. G. M. Mileo, S. Devautour-Vinot, G. Mouchaham, F. Faucher, A. Vimont and G. Maurin, *J. Phys. Chem. C*, 2016, **120**, 28374.

24 B. Saccoccia, N. W. Waggoner, K. Cho, S. Lee, D. Hong, M. Alisha, V. M. Lynch, J. Chang and S. M. Humphrey, *Angew. Chem., Int. Ed.*, 2015, **54**, 5394.

25 J. Woong, S. H. Jhung, Y. K. Hwang, S. M. Humphrey, P. T. Wood and J.-S. Chang, *Adv. Mater.*, 2007, **19**, 1830.

26 J. P. Perdew, K. Burke and M. Ernzerhof, *Phys. Rev. Lett.*, 1996, **77**, 3865.

27 (*a*) W. J. Hehre, J. A. Ditchfield and J. A. Pople, *J. Chem. Phys.*, 1972, **56**, 2257; (*b*) C. Campañá, B. Mussard and T. K. Woo, *J. Chem. Theory Comput.*, 2009, **5**, 2866.

28 J. G. Harris and K. H. Yung, *J. Phys. Chem.*, 1995, **99**, 12021.

29 J. L. F. Abascal and C. Vega, *J. Chem. Phys.*, 2005, **123**, 234505.

30 G. Kamath, N. Lubna and J. J. Potoff, *J. Chem. Phys.*, 2005, **123**, 124505.

31 A. K. Rappe, C. J. Casewit, K. S. Colwell, W. A. Goddard and W. M. Skiff, *J. Am. Chem. Soc.*, 1992, **114**, 10024.

32 S. L. Mayo, B. D. Olafson and W. A. Goddard, *J. Phys. Chem.*, 1990, **94**, 8897.

33 (*a*) E. Sánchez-González, P. G. M. Mileo, J. R. Álvarez, E. González-Zamora, G. Maurin and I. A. Ibarra, *Dalton Trans.*, 2017, **46**, 15208; (*b*) D. D. Borges, P. Normand, A. Permiakova, R. Babarao, N. Heymans, D. S. Galvão, C. Serre, G. De Weireld and G. Maurin, *J. Phys. Chem. C*, 2017, **121**, 26822.

34 (*a*) O. N. Osychenko, G. E. Astrakharchik and J. Boronat, *Mol. Phys.*, 2012, **110**, 227; (*b*) J. Kolafa and J. W. Perram, *Mol. Simul.*, 1992, **9**, 351.

35 T. J. H. Vlugt, E. García-Perez, D. Dubbeldam, S. Ban and S. Calero, *J. Chem. Theory Comput.*, 2008, **4**, 1107.

36 (*a*) H. Kim, S. R. Rao, E. A. Kapustin, L. Zhao, S. Yang, O. M. Yaghi and E. N. Wang, *Nat. Commun.*, 2018, **9**, 1191; (*b*) H. Kim, S. Yang, S. R. Rao, S. Narayanan, E. A. Kapustin, H. Furukawa, A. S. Umans, O. M. Yaghi and E. N. Wang, *Science*, 2017, **356**, 430.

37 A. Cadiau, J. S. Lee, D. D. Borges, P. Fabry, T. Devic, M. T. Wharmby, C. Martineau, D. Foucher, F. Taulelle, C.-H. Jun, Y. K. Hwang, N. Stock, M. F. De Lange, F. Kapteijn, J. Gascon, G. Maurin, J.-S. Chang and C. Serre, *Adv. Mater.*, 2015, **27**, 4775.

38 A. J. Rieth, S. Yang, E. N. Wang and M. Dincă, *ACS Cent. Sci.*, 2017, **3**, 668.

39 (*a*) J. R. Álvarez, R. A. Peralta, J. Balmaseda, E. González-Zamora and I. A. Ibarra, *Inorg. Chem. Front.*, 2015, **2**, 1080;

 

(*b*) E. Sánchez-González, J. R. Álvarez, R. A. Peralta, A. Campos-Reales-Pineda, A. Tejeda-Cruz, E. Lima, J. Balmaseda, E. González-Zamora and I. A. Ibarra, *ACS Omega*, 2016, **1**, 305; (*c*) R. A. Peralta, B. Alcántar-Vázquez, M. Sánchez-Serratos, E. González-Zamora and I. A. Ibarra, *Inorg. Chem. Front.*, 2015, **2**, 898.

40 (*a*) X. Zhao, B. Xiao, A. J. Fletcher, K. M. Thomas, D. Bradshaw and M. J. Rosseinsky, *Science*, 2004, **306**, 1012; (*b*) H. J. Choi, M. Dincă and J. R. Long, *J. Am. Chem. Soc.*, 2008, **130**, 7848.

41 R. Roque-Malherbe, *Microporous Mesoporous Mater.*, 2000, **41**, 227.

42 R. A. Peralta, A. Campos-Reales-Pineda, H. Pfeiffer, J. R. Álvarez, J. A. Zárate, J. Balmaseda, E. González-Zamora, A. Martínez, D. Martínez-Otero, V. Jancik and I. A. Ibarra, *Chem. Commun.*, 2016, **52**, 10273.

43 (*a*) D.-M. Chen, X.-P. Zhang, W. Shi and P. Cheng, *Inorg. Chem.*, 2015, **54**, 5512; (*b*) G. E. Cmarik, M. Kim, S. M. Cohen and K. S. Walton, *Langmuir*, 2012, **28**, 15606; (*c*) D.-M. Chen, N.-N. Zhang, C.-S. Liu, Z.-H. Jiang, X.-D. Wang and M. Du, *Inorg. Chem.*, 2017, **56**, 2379.

44 (*a*) A. C. Kizzie, A. G. Wong-Foy and A. J. Matzger, *Langmuir*, 2011, **27**, 6368; (*b*) J. A. Mason, T. M. McDonald, T.-H. Bae, J. E. Bachman, K. Sumida, J. J. Dutton, S. S. Kaye and J. R. Long, *J. Am. Chem. Soc.*, 2015, **137**, 4787; (*c*) V. Benoit, N. Chanut, R. S. Pillai, M. Benzaqui, I. Beurroies, S. Devautour-Vinot, C. Serre, N. Steunou, G. Maurin and P. L. Llewellyn, *J. Mater. Chem. A*, 2018, **6**, 2081.

45 S. Vaesen, V. Guillerm, Q. Yang, A. D. Wiersum, B. Marszalek, B. Gil, A. Vimont, M. Daturi, T. Devic, P. L. Llewellyn, C. Serre, G. Maurin and G. De Weireld, *Chem. Commun.*, 2013, **49**, 10082.

46 Y. Hijikata, S. Horike, D. Tanaka, J. Groll, M. Mizuno, J. Kim, M. Takata and S. Kitagawa, *Chem. Commun.*, 2011, **47**, 7632.

47 (*a*) Y. Laligant, A. Le Bail and F. Goutenoire, *J. Solid State Chem.*, 2001, **159**, 223; (*b*) T. Riosnel, J. Gonzalez-Platas and J. Rodriguez-Carvajal, *WinPlotr and FullProf suite program, version 3.00*, 2015, https://www.ill.eu/sites/fullprof, (june, 2017).

48 Q. Yang, S. Vaesen, M. Vishnuvarthan, F. Ragon, C. Serre, A. Vimont, M. Daturi, G. De Weireld and G. Maurin, *J. Mater. Chem.*, 2012, **22**, 10210.